

PVP2009-77320

ANALYSIS OF CONTACT PRESSURE DISTRIBUTION ON 3-BOLT SELF-ENERGIZED CONNECTOR SEALS

Rajeev Madazhy
Taper-Lok Corporation
Houston, Texas

Sheril Mathews
Taper-Lok Corporation
Houston, Texas

Erik Howard
Taper-Lok Corporation
Houston, Texas

ABSTRACT

A novel design using 3 bolts for a self-energized seal connector is proposed for quick assembly applications. Contact pressure distribution on the surface of the seal ring during initial bolt-up and subsequent operating pressure is analyzed for 3" and 10" connectors using Finite Element Analysis. FEA is performed on a 3" and 10" ANSI RF flange assembly and contact pressure distribution on the RF gasket is compared with the tapered seal ring assemblies. Hydrostatic tests are carried out for the tapered seal and ANSI bolted connectors to evaluate maximum pressure at which leak occurs for both size assemblies.

INTRODUCTION

3-Bolt connector was designed to meet the requirements of quick assembly, misalignment and swivel capabilities. The connector uses self-energized seal technology. The seal ring has converging double-tapered angles. The 10° and 20° angle design is driven by the basic wedge principle as shown in Figure 1. The male member and the seal ring have mating annular spherical surfaces which are respectively convex and concave [1]. The female member and seal ring has mating frusto-conical tapered surfaces as shown in Figure 2, but the outside diameter of the seal ring is slightly larger than the inside diameter of the female sealing surface. The seal ring wedges itself between the male nose and female pocket due to the tapered angles and the bolts push the surfaces against each other, resulting in a compressive hoop stress. These angles also leverage the bolt load to achieve high resultant loads at the

sealing surface, which translate into high contact pressures. Prior to drawing the male and female members together by bolting respective flanges, the convex male member surface is pivotably engaged with the concave seal ring surface for alignment of the members in the desired swiveled position. The radial compression produces a seal between the male and female members and the seal ring, and locks the members into the swiveled alignment. Misalignment flanges were first used in sub-sea applications, where pipelines were not co-axial. Watts used the misalignment design in a multi-piece line and elbow assembly [2] for plant applications.

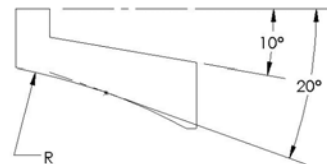


Fig. 1 Seal Ring Geometry

A "doorstop" effect is created when internal pressure builds up behind the seal ring and drives the wedge further. The connector is also designed to misalign up to 3° and the swivel flange allows for 360° axial pipe rotation. The seal ring is made of the same material as the flanges to ensure that, thermal expansion is consistent across all sealing components and bimetallic corrosion is eliminated. Kodner [3] et al. did some preliminary analytical work on tapered seal flange joints using converging seal surfaces with a round seal ring. Their work

demonstrated the advantages of high contact pressure at the pressure-energized condition. More recently, Kurokouchi [4] et al. evaluated seal reliability with a tapered seal for ultrahigh vacuum systems as compared to conventional disk gasket. The authors highlighted the advantage of the area seal requiring lesser torque at bolt-up and having a more uniform seal pressure distribution. Another feature highlighted was the reusability of tapered-seal gaskets.

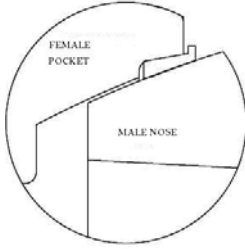


Fig. 2 Section Showing Male Nose and Female Pocket

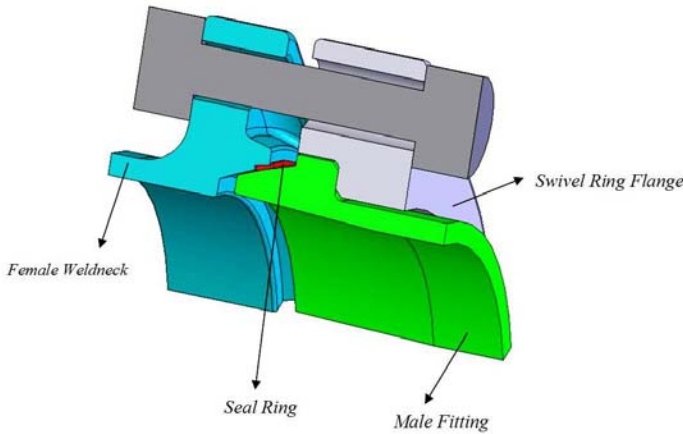


Fig. 3 Section of 3-Bolt Misalignment Swivel Flange

NOMENCLATURE

- θ_m = Male Taper Angle = 20°
 θ_f = Female Taper Angle = 10°
 μ = Max. Co-efficient of Friction = 0.2
 H = Total Hydrostatic End Force
 T_{sr} = Compressive Force in Seal Ring
 f_m = Max. Friction Force on Male Surface
 f_f = Max. Friction Force on Female Surface
 N_m = Max. Normal Force on Male Surface
 N_f = Max. Normal Force on Female Surface
 σ_{mc} = Average Contact Pressure on Male Surface

σ_{fc} = Average Contact Pressure on Female Surface

G = ANSI Gasket Diameter

P = Internal Design Pressure

G_f = Female Gasket Diameter

G'_D = Deformed Seal Ring Diameter

G_m = Male Gasket Diameter

FORMULATION

The total hydrostatic end force H as per ASME Section VIII Div. 1 Appendix 2 [5] code is given by

$$H = 0.785G^2P \quad (1)$$

The maximum normal force N_m on male surface is given by

$$N_m = \frac{H}{\sin\theta_m + \mu\cos\theta_m} \quad (2)$$

The maximum normal force N_f on female surface is given by

$$N_f = \frac{2\pi T_{sr} + N_m \cos\theta_m - f_m \sin\theta_m}{\cos\theta_f - \mu\sin\theta_f} \quad (3)$$

The average contact pressure σ_{fc} on female surface is determined as follows

$$\sigma_{fc} = \frac{N_f \sin\theta_f}{\pi/4(G_f^2 - G_D^2)} \quad (4)$$

The corresponding average contact pressure σ_{mc} on male surface is given by

$$\sigma_{mc} = \frac{N_m \sin\theta_m}{\pi/4(G_D^2 - G_m^2)} \quad (5)$$

FINITE ELEMENT ANALYSIS

Non-linear finite element analysis was performed to calculate the contact pressure distribution between the male and female sealing surfaces. Figure 4 shows the stress strain curve for SA-105 obtained by tension test [9]. Table 1 lists the material properties of SA-105 and SA-193 B7. Finite element models for the tapered seal geometry included five components: male fitting, seal ring, swivel flange, female weldneck flange and the bolt. Commercially available finite

element analysis software package, ABAQUS [7] was used for calculations.

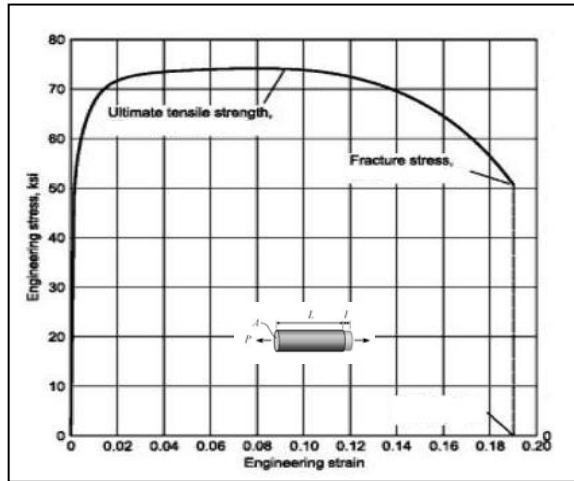


Fig. 4 Stress Strain Curve for SA-105 Material

Table 1 Material Properties from Tension Test

Material	Yield Strength-0.2% Offset (psi)	Ultimate Tensile Strength (psi)	Elongation
SA-105	47,553	74,002	37%
SA-193 B7	127,134	139,957	17%

Model Geometry

Two nominal pipe sizes of the 3-Bolt flanges were modeled: 3” and 10”. Each part was modeled using SA-105 and bolt using SA-193 B7 carbon steel properties. Table 2 summarizes pertinent geometric dimensions for both sizes. The 3” and 10” ANSI RF flange assemblies were considered with 3 bolts to study and compare the contact pressure distribution with that of tapered seal assembly. The geometric modeling was done using SolidWorks and meshing, definition of boundary conditions, loads during bolt-up and internal pressure were applied using ABAQUS CAE package.

Figure 3 shows a one-sixth solid model of the assembly, color coded to distinguish individual components. 3D solid continuum elements: C3D4 (4-node linear tetrahedron) and C3D8 (8-node linear brick) were used in the analysis. Brick elements were used at sealing surfaces for their better efficiency and convergence behavior in highly non-linear problems. In order to keep the number of elements reasonable and yet provide sufficient refinement to generate accurate results, symmetry conditions were invoked. Figures 5 and 7 show finite element mesh of tapered seal and ANSI bolted flange assembly respectively.

Boundary Conditions and Loading

Figure 6 shows boundary conditions and loads on the model. The pre-tension feature was used in ABAQUS to load the bolt. For these analyses, bolts were given a pre-stress value of 25,000 psi. Pressure loads were applied on the inside surfaces of the flange and the seal ring and hydrostatic end load was applied at the end of the pipe. Internal pressure of 285 psi (ANSI 150#) was considered for both sizes.

Table 2 Tapered Seal Flange Dimensions

Pipe Size (in.)	Bolt Size (in.)	Female Flange Thickness (in.)	Ring Flange Thickness (in.)	Bolt Circle Diameter (in.)
3”	5/8”	0.940”	1.250”	5.750”
10”	7/8”	1.500”	2.000”	14.125”

The following steps were used in the ABAQUS analysis:

1. Apply pre-tension load to the bolt
2. Apply hydrostatic end load and internal pressure

The pre-tension load of each bolt is applied at the beginning of the first step, and the bolt length is fixed after tightening, so that changes in bolt tension can be captured during internal pressure step.

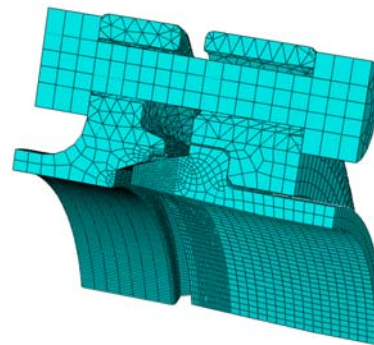


Fig. 5 Typical Finite Element Mesh of 3-Bolt Flange Assembly

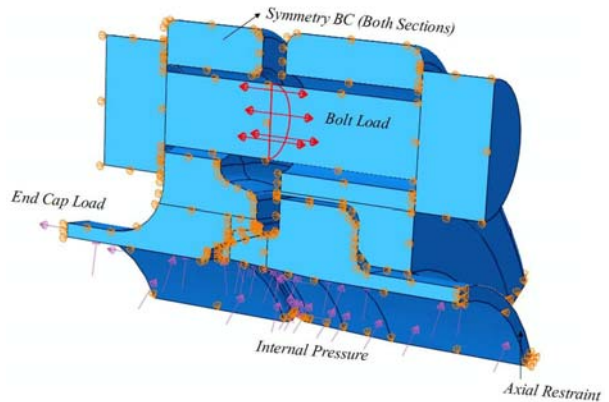


Fig. 6 Boundary Conditions and Loading for 3-Bolt Flange Assembly

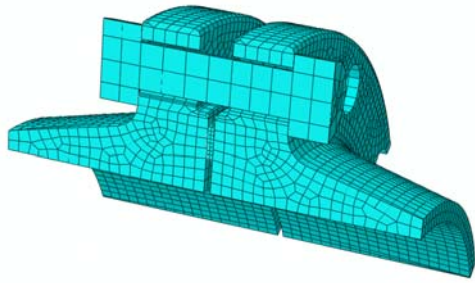


Fig. 7 Typical Finite Element Mesh of 3-Bolt ANSI Flange Assembly

Cases Analyzed

Four cases were analyzed. Case 1 and 2 used 3” and 10” 3-bolt tapered seal assembly respectively. Case 3 and 4 involved using 3” and 10” 3-bolt ANSI flange assembly. For all four cases, contact pressure distribution across the sealing surface was examined and quantified.

Analysis Results and Commentary

Finite element results are presented using color contour plots. Figure 8 shows the von Mises stress distribution on the 3” 3-bolt assembly. Figures 9 and 12 show the contact distribution on the female and male side of seal ring respectively. Figure 10 and 13 show a path selected on male and female side of the seal ring to evaluate the contact pressure distribution. The true distance across the length of the sealing surface is selected for evaluating all contact pressure distributions. Figures 11 and 14 show the contact distribution plotted against distance on the female and male surface of the seal ring respectively. Figures 15, 16, 17, 18, 19, 20, 21 and 22 illustrate the same for the 10” 3-bolt assembly.

Figures 23, 24, 25, and 26 depict as mentioned above for the 3” 3- bolt ANSI assembly and Figures 27, 28, 29 and 30 depict the same for the 10” 3- bolt ANSI assembly.

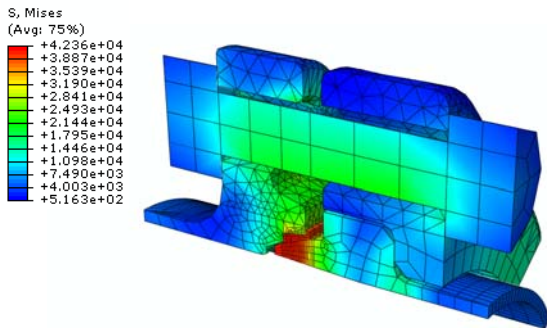


Fig. 8 von Mises Stress Distribution on 3” 3-Bolt Assembly

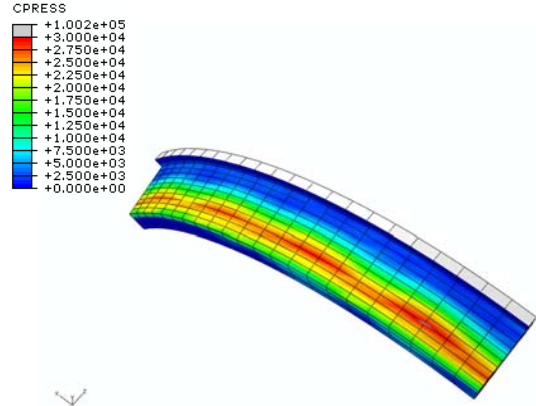


Fig. 9 Contact Pressure Distribution on 3” 3-Bolt Seal Ring (Female Side)

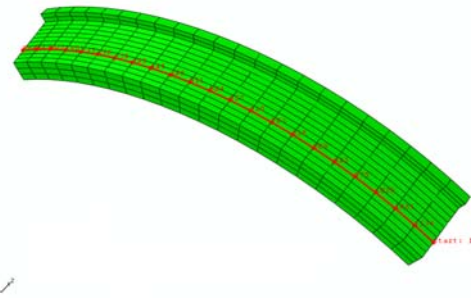


Fig. 10 Typical Path across Female Surface on 3” 3-Bolt Seal Ring

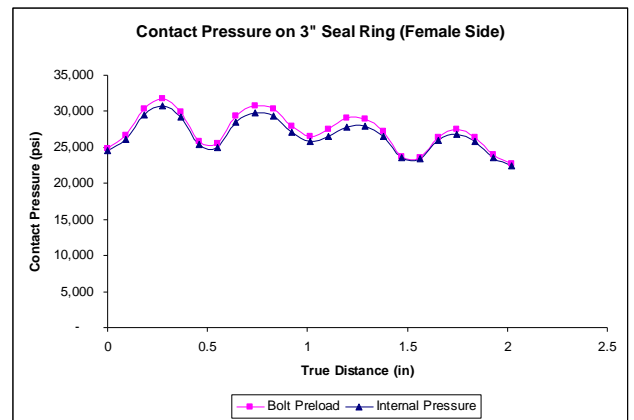


Fig. 11 Contact Pressure Distribution along Selected Path (Female Side)

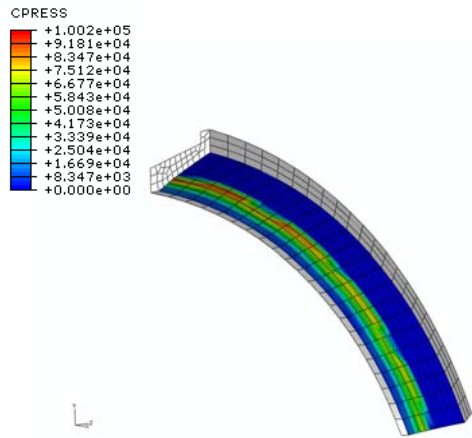


Fig. 12 Contact Pressure Distribution on 3" 3-Bolt Seal Ring (Male Side)

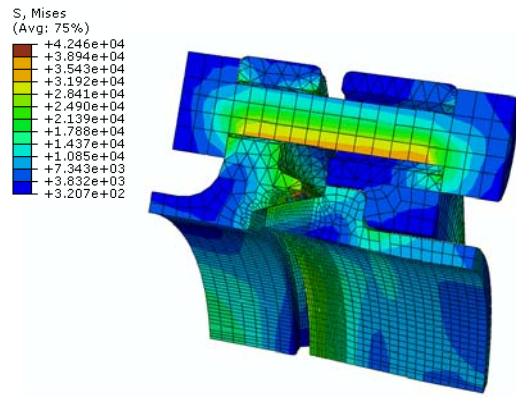


Fig. 15 von Mises Stress Distribution on 10" 3-Bolt Assembly

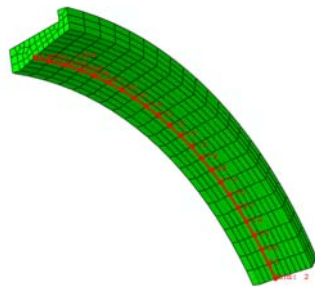


Fig. 13 Typical Path across Male Surface on 3" 3-Bolt Seal Ring

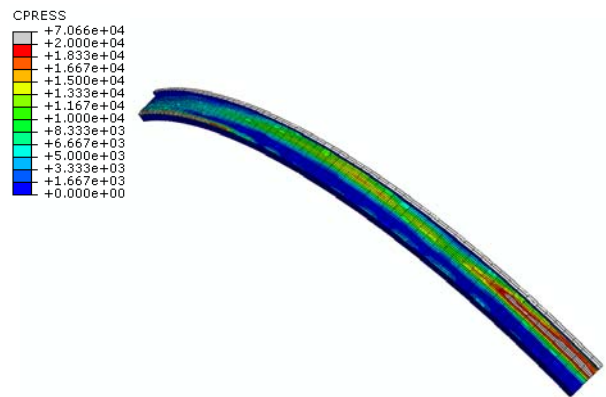


Fig. 16 Contact Pressure Distribution on 10" 3-Bolt Seal Ring (Female Side)

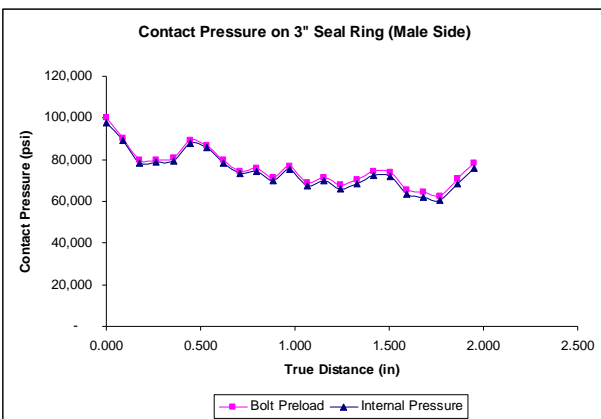


Fig. 14 Contact Pressure Distribution along Selected Path (Male Side)

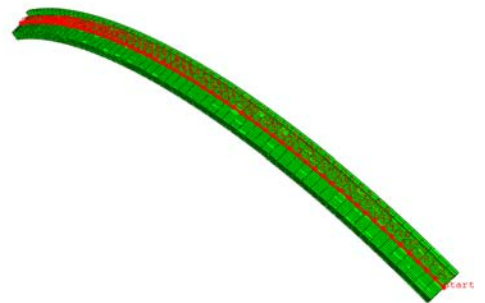


Fig. 17 Typical Path across Female Surface on 10" 3-Bolt Seal Ring

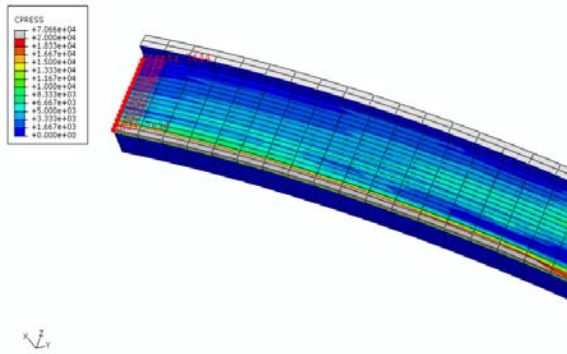


Fig. 18 Path across Width of Seal Ring Farthest Away From Bolt

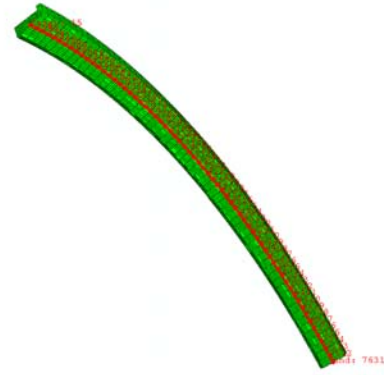


Fig. 21 Typical Path across Male Surface on 10" 3-Bolt Seal Ring

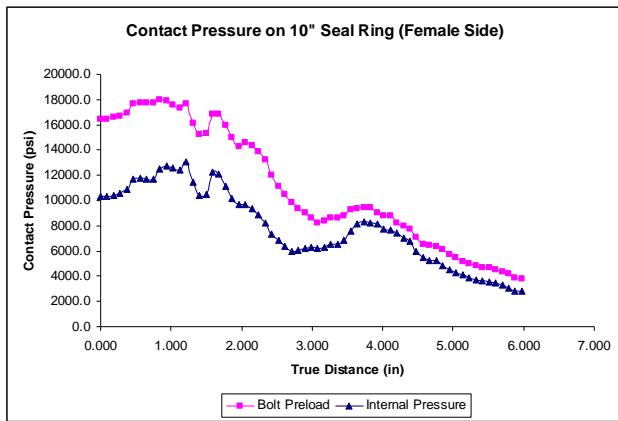


Fig. 19 Contact Pressure Distribution along Selected Path (Female Side)

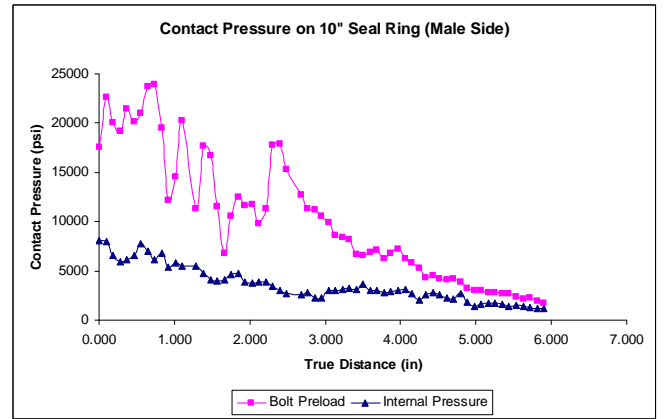


Fig. 22 Contact Pressure Distribution along Selected Path (Male Side)

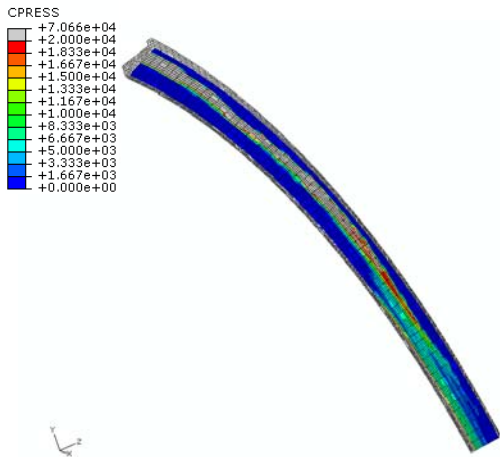


Fig. 20 Contact Pressure Distribution on 10" 3-Bolt Seal Ring (Male Side)

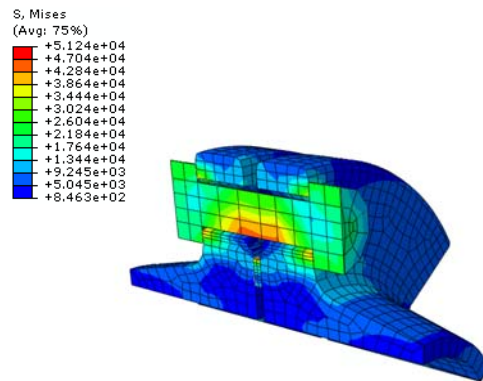


Fig. 23 von Mises Stress Distribution on 3" 3-Bolt ANSI Assembly

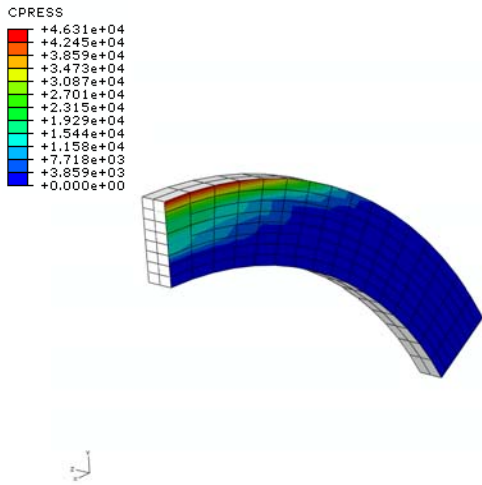


Fig. 24 Contact Pressure Distribution on 3" 3-Bolt ANSI RF Gasket

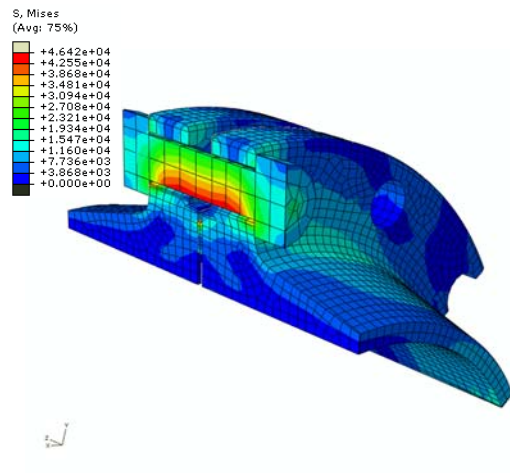


Fig. 27 von Mises Stress Distribution on 10" 3-Bolt ANSI Assembly

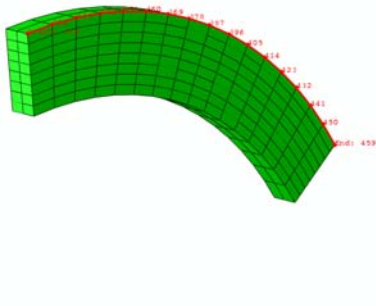


Fig. 25 Typical Path across 3" 3-Bolt ANSI RF Gasket Surface

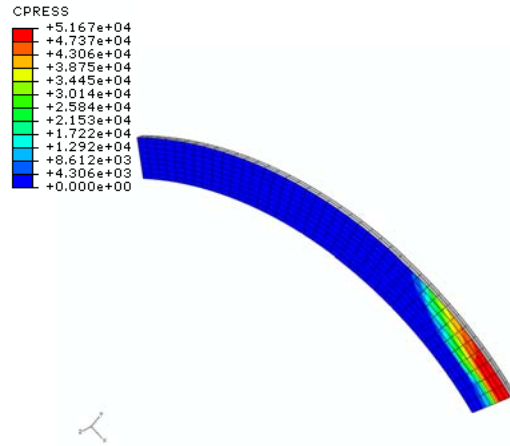


Fig. 28 Contact Pressure Distribution on 10" 3-Bolt ANSI RF Gasket

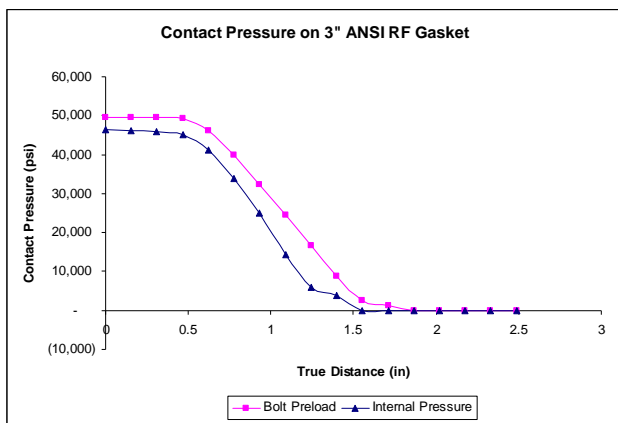


Fig. 26 Contact Pressure Distribution along Selected Path (ANSI RF Gasket)

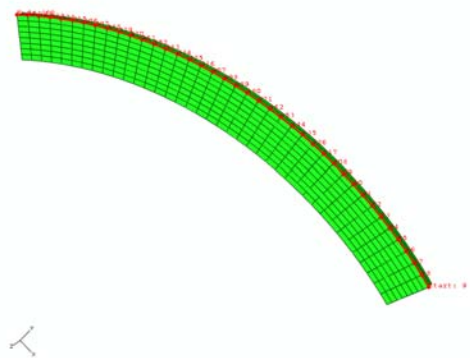


Fig. 29 Typical Path across 10" 3-Bolt ANSI RF Gasket Surface

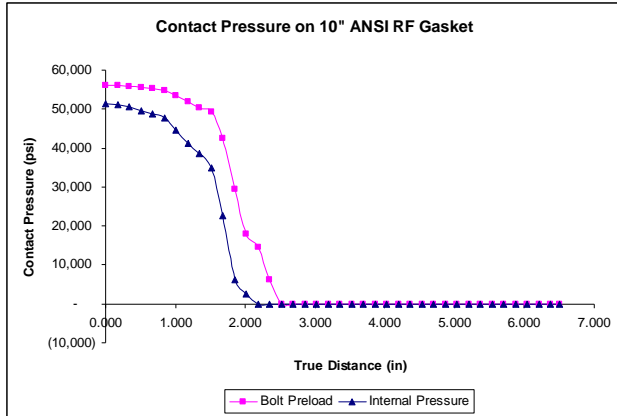


Fig. 30 Contact Pressure Distribution along Selected Path (ANSI RF Gasket)

It is noted that the contact pressure distribution as seen in Figure 11 for the 3" seal ring (female side) is reasonably uniform across the sealing surface with an average contact pressure of 26,600 psi. There is 9% difference in contact pressure on the seal ring between points closest and farthest away from the bolt, when internal pressure is applied. Figure 14 shows the contact pressure distribution on the 3" seal ring (male side) with an average contact pressure of 75,780 psi. The differences in contact pressures between the female and male surfaces are attributed to different shallow angles and higher contact pressures on the male surface due to smaller contact area on the spherical surface. Figures 19 and 22 show plots of contact pressure distribution on the female and male side of the 10" seal ring respectively, when internal pressure is applied. On the female side, there is a 72% difference in contact pressure between points farthest away from each other on the selected path. On the male side, there is an 80% difference in contact pressure for the same two points. It is observed that even though the contact pressure at the furthest point on the female side on the selected path is 2,800 psi, the highest value across the width of the sealing surface (Figure 18) at that same point was 7,840 psi. The average contact pressure across the path evaluated was 4,560 psi. The same phenomenon is observed on the male side too, which highlights the presence of sufficient contact pressure, though non uniform in nature. Figures 26 and 30 show the contact pressure distribution along the 3" and 10" ANSI RF gasket for both bolt up and internal pressure. It is observed that even though there is a very high contact pressure below the bolt, it drops very quickly to zero across the gasket.

HYDROTEST

Hydrotest was performed for 3 cases as shown in Table 3. Kammpofile gasket was used for the 10" 3-bolt ANSI assembly. For both the tapered seal ring assemblies, a bolt pre-

stress of 25,000 psi was applied, since the seal ring is pressure-energized [8] and no sealing load is required. For the 10" ANSI assembly, 50,000 psi bolt pre-stress was applied. The two tapered seal ring flange assemblies sealed at 427.5 psi hydrotest pressure (Figure 31). For the 10" ANSI flange assembly (Figure 32), even though the rated hydrotest pressure was 427.5 psi, the connection leaked at 220 psi. Table 3 tabulates the pressures at which leakage occurred for the assemblies.



Fig. 31 10" 3-Bolt Assembly



Fig. 32 10" 3-Bolt ANSI Assembly

Table 3 Hydrotest Leakage Pressures for 3 Cases

Size (in)	Bolt Pre-stress (psi)	Hydrotest Pressure (psi)	Leakage Pressure (psi)
3" 3-Bolt assembly	25,000	427.5	2,800
10" 3-Bolt assembly	25,000	427.5	1,200
10" ANSI 3-bolt assembly	50,000	-	220

CONCLUSIONS

The contact distribution for 3" and 10" tapered seal ring and the 10" ANSI RF assemblies were analyzed. Contact distribution on the 3" tapered seal ring was larger and more uniform compared to the 10" seal ring. It was also noted that for the 10" connection, there was enough contact pressure on the tapered seal ring farthest away from the bolt.

There was no contact pressure at the same location on the ANSI RF gasket. Hydrotest conducted on the two tapered seal assemblies demonstrated the ability to seal at 427.5 psi and only leaked at higher pressures as compared to an ANSI assembly with 3 bolts. The authors acknowledge that for ANSI assemblies, having all the bolts provides a suitable seal at specified pressures. Analyzing with just 3 bolts on an ANSI flange assembly was to demonstrate the absence of contact pressure further away from the bolt. The difference in contact pressure distributions between the tapered seal ring and ANSI assemblies was the presence of wedge geometry, resulting in sufficient contact pressure across the tapered seal ring, a result of high contact forces that exist between the surfaces, as compared to sparse contact pressure on a flat gasket surface. It must be noted though, that a limit might be reached with the 10" tapered seal ring connection because of highly non uniform pressure distribution across the surface of the seal ring and would require 4 bolts for higher sizes.

REFERENCES

- [1] *Swivel Flow Line Connector*, Joseph J. Welkey, Taper-Lok Corporation, United States Patent# 4840409, 1989
- [2] *Multiple-Piece Elbow Assembly*, Kenneth A. Watts, Taper-Lok Corporation, United States Patent# 6279964, 2001
- [3] *Method for Calculating Tapered-Sealed Flange Joints*, M. Ya. Kodner, A.N Chekalin, J. of Strength of Materials, Springer, Volume 1/Number 5, 1969
- [4] *Taper-seal Type Metal Sealing System and Available Applications*, Satoshi Kurokouchi, Masayuki Okabe, Shinsaku Morita, Applied Surface Science 169-170, 2001.
- [5] *ASME Boiler & Pressure Vessel Code, Section VIII Division I, Appendix 2*, American Society of Mechanical Engineers, New York, 2007
- [6] *Areas of Contact and Pressure Distribution in Bolted Joints*, H.H. Gould, B.B.Mikic, Technical Report, 1970
- [7] *ABAQUS V6.8. User's Manual*, Dassault Systèmes, 2008
- [8] *High Pressure Heat Exchanger Diaphragm Removal/Retrofit Using Double Tapered Pressure Seal*, D Hughes, J Cesarini, E Howard, NPRA Reliability & Maintenance Conference, Houston, 2007
- [9] *SA-105 Tension Test Report*, AFG Metallurgical Lab, Houston, TX, 2008